phys. stat. sol. (b) **220**, 845 (2000)

Subject classification: 61.72.Yx; S1.1; S1.3

Atomistic Simulations of Interactions between Cu Precipitates and an Edge Dislocation in a B.C.C. Fe Single Crystal

S. Y. HU (a), S. SCHMAUDER (b), and L. Q. CHEN (a)

(a) Department of Materials Science and Engineering, The Pennsylvania State University, University Park, PA 16802, USA

(b) Staatliche Materialprüfungsanstalt (MPA), University of Stuttgart, Pfaffenwaldring 32, D-70569 Stuttgart, Germany

(Received November 1, 1999; in revised form April 25, 2000)

Interactions between precipitates and dislocations were investigated using atomistic computer simulations. In particular, the effect of Cu precipitates on the core structures, slipping behavior, and Critical Resolved Shear Stress (CRSS) of an edge dislocation in a b.c.c. Fe single crystal was considered. Three-dimensional (3D) molecular statics were performed on a $a_0/2(110)$ [111] edge dislocation passing through spherical Cu precipitates under shear deformations. The atomic stresses on the dislocation slip plane are calculated for different deformation stages. The characteristics of stress distributions and dislocation core structures are analyzed. The Peierls stress of a pure edge dislocation and the CRSS in the presence of Cu precipitates are determined. Finally, the mechanisms of the dislocation passing through Cu precipitates were analyzed by examining the evolution of atomic configurations.

1. Introduction

The effect of fine Cu precipitates on the core structures and slipping behaviors of dislocations is of importance to the understanding of irradiation embrittlement of pressure vessels. Experimental investigations [1, 2] suggested that coherent b.c.c. Cu precipitates nucleate and grow in the Cu-supersaturated matrix under electronic irradiation or during thermal aging. During growth, Cu precipitates undergo complex structural transformations: coherent b.c.c. 9R$\rightarrow$ 3R $\rightarrow$ f.c.c. Similar structural transformations in Cu precipitate can be induced by an applied stress or in a dislocation stress field [3, 4]. These transformations are accompanied by volume and shape changes of Cu precipitates. The coherent lattice accommodation between the Cu precipitates and the Fe matrix leads to an internal stress field around Cu precipitates. In the presence of dislocations, the coherency stress field produced by the precipitates interacts with those of dislocations. Therefore, the presence of coherent precipitates affects the core structures and slipping behaviors of dislocations, and hence, the material mechanical properties. Indeed, experimental evidences suggested that there is a strong correlation between the strength change of these materials and the presence of fine b.c.c. Cu precipitates (2 to 4 nm).

Precipitate-hardening mechanisms of alloys have been extensively investigated for decades by both experimental and theoretical methods (see, for example, references [5, 6], for reviews). To determine quantitatively the contribution of precipitates and particles to the material embrittlement, a number of hardening mechanisms have been pro-

posed, such as modulus mismatch hardening, coherency strain hardening, chemical hardening, and so on. These mechanisms have been used to explain the strength of some related alloys [6]. However, it should be emphasized that confirmation of various hardening mechanisms and validation of theoretical models are quite difficult, since ideal alloys systems, which most of the theoretical models assumed, are rarely available in practical applications, and in many cases more than one hardening mechanisms are operative [6]. For example, currently there is no physically based theoretical model available to explain the Cu precipitate-hardening in Fe.

It is well known, plastic properties of a material rely on the core structures and mobility of dislocations. Atomistic simulation methods such as molecular dynamics and lattice statics have been successfully employed to study the dislocation core structures [7 to 13]. However, as far as the authors are aware of, there have been no atomistic simulation studies on the effect of precipitate particles on the dislocation core structures, the atomic mechanisms of a dislocation passing through a precipitate, and on the CRSS. It should be pointed out that one of the main advantages of atomistic techniques is the fact that it automatically includes the modulus mismatch between precipitate and matrix, coherency strain, and interfacial energy between precipitate and matrix. Therefore, it is an obvious choice of theoretical methods for studying the CRSS of precipitate strengthening in metals and alloys with small-size precipitates, such as the case of Cu precipitates in Fe single crystal, so that current generation of computers will be able to handle the memory and computation requirement. In this paper, we apply the molecular static relaxation method to study Cu precipitate strengthening with embedded atom potentials. The interaction between spherical Cu precipitates and an $a_0/2(1\bar{1}0)$ [111] edge dislocation in a b.c.c. Fe single crystal is considered. The effect of precipitates on the structure of a dislocation core is analyzed. The behavior of a dislocation passing through the precipitate under an applied shear stress is simulated. By comparing with the slipping of a pure dislocation, the contribution of precipitates to CRSS is discussed.

2. Computational Procedure

The atomic model employed in the present work is shown in Fig. 1. It includes an approximately spherical b.c.c. Cu precipitate with a diameter D_0 and a straight $a_0/2(1\bar{1}0)$ [111] edge dislocation in a b.c.c. Fe matrix. The x, y and z coordinate axes are lying along crystal directions [111], $[1\bar{1}0]$ and $[11\bar{2}]$, respectively. Periodic boundary conditions are applied in the x and z directions. Therefore, the dislocation has an infinite length along the z direction, and the Cu precipitates are periodically distributed. Along

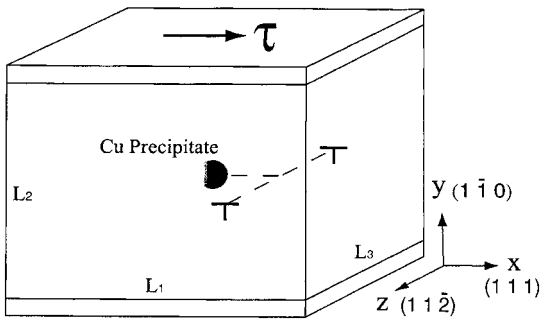

Fig. 1. Model of a b.c.c. Fe single crystal with an edge dislocation and a Cu precipitate under shear deformation

y direction, the model is divided into two regions, i.e., an active region and a boundary region. The central part of the model is the active region in which atoms are specifically relaxed to the equilibrium positions according to the interatomic potentials using a static relaxation method. The size of the active region is indicated by L_1, L_2 and L_3 in Fig. 1. $L_1 = 40\,a_0$ to $48\,a_0$ and $L_2 = 26\,a_0$ and $L_3 = 30\,a_0$ are chosen in the present work, where $a_0 = 2.876$ Å is the lattice constant of a b.c.c. Fe single crystal. The upper and lower blocks in the model are called boundary regions. The atoms in the boundary regions possess two functions: 1. they can be used to specify a deformation with a given displacement boundary condition; and 2. they act as neighbor atoms to the active atoms for calculating the interatomic forces. During a simulation, all the atoms in the boundary regions are assigned a common displacement prescribed by a corresponding deformation process, while maintaining the atomic configuration of a perfect crystal. For example, in the present work, a pure shear deformation process is performed by displacing the atoms in the upper block with a magnitude Δu_x while fixing the atoms in the lower block. The total number of atoms in the model is about 80000 with about 50000 in the active region. The total number of atoms include those in the boundary regions in y direction and periodic boundary regions in x and z directions.

To describe the interatomic interactions, we employed the embedded atom potentials for Fe–Fe, Cu–Cu and Fe–Cu. In the embedded atom method (EAM), the potential energy E_i of an atom in the crystal is of the form

$$E_i = F_i(\varrho_i) + \tfrac{1}{2} \sum_{j(\neq i)} \varphi_{ij}^{\mathrm{AB}}(R_{ij})\,, \tag{1}$$

$$\varrho_i = \sum_{j(\neq i)} f_j(R_{ij})\,, \tag{2}$$

where the subscripts (i, j) label the i-th and j-th atoms and the superscripts (A, B) denote atom types, respectively. For a chosen atom i, j runs over all atoms in the crystal. ϱ_i is the ambient electron density at atom i and F_i is the energy required to embed atom i into electron density ϱ_i. $\varphi_{ij}^{\mathrm{AB}}(R_{ij})$ is the pair interaction potential between atom i and atom j. f_j is the electron density generated by atom j at a distance R_{ij} from its core and R_{ij} is the distance between the i-th and j-th atoms. The detailed potential forms and potential parameters were given by Simonelli et al. [14] for Fe–Fe, by Voter [15] for Cu–Cu, and by Ludwig et al. [16] for Fe–Cu.

In order to study the effect of Cu precipitates on the core structure and the slipping behavior of a $a_0/2(1\bar{1}0)$ [111] edge dislocation, we studied two cases: the movement of an edge dislocation with and without the presence of a Cu precipitate under an applied shear deformation. The dislocation core structures and the profile of the dislocation line during slipping are analyzed. The atomic stress distributions on the dislocation slip plane are calculated. Average stress–strain curves as well as CRSS are obtained.

3. Stress Calculation

Atomic stresses can be evaluated from the strain energy density W according to

$$\sigma_{kl} = \frac{\partial W}{\partial \varepsilon_{kl}}\,, \tag{3}$$

where ε_{kl} are the components of the strain tensor. The strain energy density W associated with an atom at position x_i is defined as

$$W(x_i) = \frac{E(x_i) - E_0}{\Omega}\,, \tag{4}$$

where $E(x_i)$ and E_0 are the equilibrium energies of an atom in a deformed crystal and in a perfect stress-free crystal, respectively. They are calculated using the interatomic potentials described by equation (1). $E(x_i) - E_0$ is the excess energy of a deformed crystal compared to a perfect stress-free crystal. Ω is the atomic volume in the deformed crystal. Following the procedure proposed by Hoagland et al. [17, 18], the atomic stress is calculated using a finite difference form,

$$\sigma_{kl} = \frac{W(x_i + \delta_i) - W(x_i - \delta_i)}{2\Delta u_{k,l}}\,, \tag{5}$$

in which $\delta_i = \Delta u_{i,j} x_j = \Delta u_{i,1} x_1 + \Delta u_{i,2} x_2 + \Delta u_{i,3} x_3$ is a small perturbation to the atom positions that result from applying a small additional, uniform displacement gradient increment of $\Delta u_{i,j}$ to the entire crystal. Correspondingly, $-\delta_i$ is due to $-\Delta u_{i,j}$. In equation (5), the assumption of $\Delta u_{k,l} = \Delta u_{l,k}$ is used. In applying equation (5) to the calculation of stress component $\sigma_{\alpha\beta}$, the $\alpha\beta$ component of the displacement gradient tensor $\Delta u_{i,j}$ is taken at a non-zero value while the others are set to zero.

This method has been used for calculating the internal stresses around transformed Cu precipitates [4]. In the present work, $\Delta u_{i,j}$ is taken to be 0.0001, and the atomic volume Ω is assumed to be a constant Ω_0 equal to the atomic volume in the Fe perfect crystal. The average lattice volume change in the Cu precipitate before and after stress-induced phase transformation, and the effect of the actual atomic volume Ω corrected by the volume strain on the stresses are analyzed in our previous paper [4]. It was shown that the assumption of a constant Ω has a negligible effect on the calculated stresses (see [4] for a detail analysis). We expect this assumption to be also valid for an edge dislocation with wide core structures.

4. Dislocation Core Structure

Dislocations can be introduced into the atomic simulation block by two methods. One is to insert or remove atomic planes according to the Burgers vector of the dislocation; the other is to assign anisotropic elastic displacements of a dislocation to the atoms in the simulation block. The latter has been employed in computer simulations of dislocation core structures, in which the atomic displacements in the boundary region are fixed according to the dislocation elastic solution from continuum elasticity. In present work, we are interested in the interaction between dislocations and precipitates, and the behavior of dislocations passing through precipitates. It is important to realize that there is an internal stress field around a b.c.c. Cu precipitate even without an applied stress. As reported in previous works [4, 21], the average stress inside a Cu precipitate (3 to 4 nm) in an Fe matrix is about -4 GPa. Therefore, there is a significant contribution to the elastic field from the coherent stresses arising from the lattice mismatch between a Cu precipitate and the Fe matrix. As a result, it is no longer suitable to adopt the elastic solution of a dislocation as the boundary condition when we consider the interaction between a dislocation and a precipitate. Since it is difficult to obtain an

analytical solution for systems involving both dislocations and precipitates, we adopted the former method to create an $a_0/2(1\bar{1}0)$ [111] edge dislocation with periodic boundary conditions in x and z directions and pre-described displacemental boundary conditions in the y direction. The purpose of using such boundary condition is to produce a pure shear deformation within the active region for simulating dislocation slip in the next section. More specifically, we first removed three (111) half atom planes ($y > 0$) at x_0. We then moved the two parts of the upper block separated by the removed planes gradually towards each other with a total displacement of $a_0/4[111]$ and $-a_0/4[111]$, respectively. Finally, we allowed the active atoms to relax to their equilibrium positions. It should be noted that the boundary condition used in the present work will induce an additional stress field in the active region if the model size is not sufficiently large. The influence of such a boundary condition on the simulation results will be discussed.

In a b.c.c. crystal, the core structures of an edge dislocation have previously been investigated through atomistic methods [7 to 10]. In all the cases studied, the cores of these dislocations were found to be planar, spread into their respective slip planes. They can be interpreted as several dissociated fractional dislocations which are confined to the same crystal plane. In order to study the effect of Cu precipitates, we consider two cases. The first case is a pure $a_0/2(1\bar{1}0)$ [111] edge dislocation, where no Cu precipitates exist in the simulation block. In the second case, the interactions between Cu precipitates and an $a_0/2(1\bar{1}0)$ [111] edge dislocation are considered as shown in Fig. 1, where the radius of the Cu precipitate is $5a_0$. The initial distance between the center of the precipitate and the center of the dislocation is $10a_0$. After relaxation of atoms into their equilibrium positions, it is found that the center of the dislocation core in the presence of a Cu precipitate shifts by a small distance to the Cu precipitate, and as a result the dislocation line is slightly bent. However, no shift of dislocation core is observed in the first case as expected. The dislocation line of the pure dislocation lies on the original $(1\bar{1}0)$ plane and remains straight parallel to the z direction. These observations suggest that the $a_0/2(1\bar{1}0)$ [111] dislocation is attracted to the coherent b.c.c. Cu precipitate. Interactions between Cu precipitates and the dislocation also lead to structure changes of the Cu precipitate and dislocation core. Figs. 2a and b present the atom-

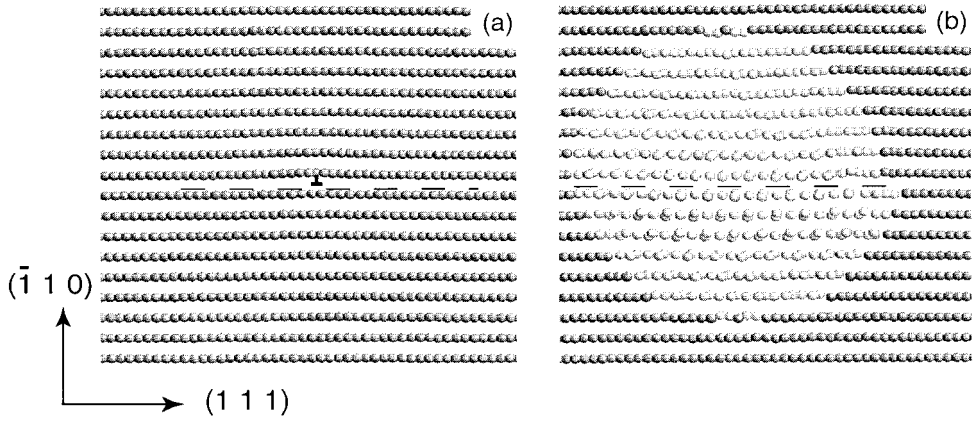

Fig. 2. Dislocation core structures on $(11\bar{2})$ plane: a) in the arm part ($z = 10\,a_0$), b) in the middle part ($z = 0$)

ic structures of the dislocation core on the $(11\bar{2})$ plane in the arm part (located at $z = 10a_0$) and the middle part (located at $z = 0$) of the dislocation, respectively. For the pure dislocation, the atomic configuration of the core structure is omitted because it is almost the same as that in Fig. 2a. From Fig. 2a, it can be seen that the core structure of the pure dislocation and the arm part of the dislocation in the presence of a precipitate is of planar configuration. They spread on the $(1\bar{1}0)$ slip plane and the dislocation core has a finite width. However, since the b.c.c. Cu precipitate is a metastable structure, the presence of the dislocation results in a structure transformation in the Cu precipitate. An obvious structure difference between the Cu precipitate and the matrix around it can be observed in Fig. 2b. The structure changes in the central region of Cu precipitate are presented in Fig. 3. It can be seen that the structure change is due to the slipping of (101) plane along $[10\bar{1}]$ direction. According to a hard-sphere model of the b.c.c. $\rightarrow$ 9R transformation proposed by Ahler [19] and Kajiwara [20], sliding of (101) planes in the $[10\bar{1}]$ direction implies that a phase transformation from b.c.c. to 9R occurs in the Cu precipitate. Similarly, this phase transformation results in a complex dislocation core structure as shown in Fig. 2b. It is rather difficult to analyze such a dislocation core structure from direct visualization of atomic configurations.

In the atomic modeling of dislocation core structures, the interpretation of results is of primary importance since the position vectors of a large number of atoms are obtained from a given simulation. To quantitatively characterize the core structure of a dislocation, one needs to define a quantity which is large in the core region and vanishes far from it. For this purpose, two methods, the mapping of differential displacements [11] and the mapping of the stress tensor at individual atoms [8], have been previously proposed. Because of the complicated dislocation core structure in our simulation as shown in Fig. 2b, it is rather impractical to interpret the dislocation core structures using the differential displacemental method. Therefore, in the present work, the stress tensor method is employed. We used the stress calculation method described in the previous section to calculate the stress components on the dislocation slip plane near the dislocation cores. The normal stress σ_{yy} and shear stress σ_{xy} are shown in Fig. 4, in which the solid line represents the stress distribution for the pure dislocation; the short-dash line for the middle part ($z = 0$) and the long-dash line for the arm part of the dislocation in the presence of a Cu precipitate. Analyzing the shear and normal stress distributions and the atomic configuration in Fig. 2a, we obtain the following results. For the pure dislocation, the dislocation core structure possesses a planar core structure, and is symmetrical with respect to the core center (defined by the position of the central peak of the solid line in Fig. 4b). There are three peaks or inflections in the normal stress distribution. A comparison between the atomic configu-

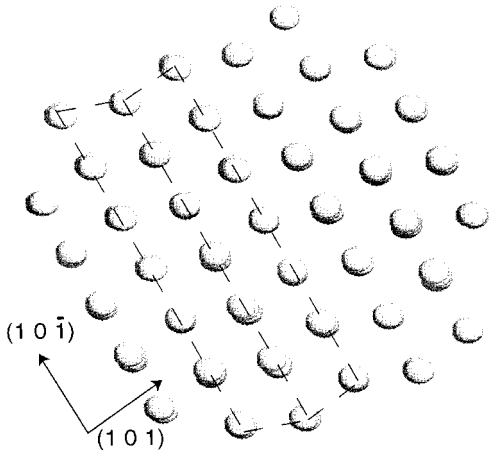

Fig. 3. Structure transformation in the center of the Cu precipitate

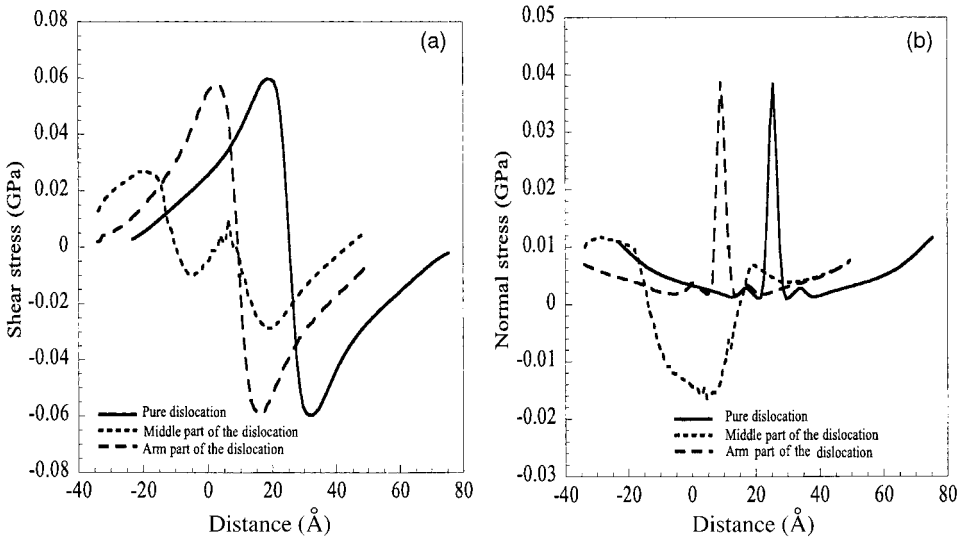

Fig. 4. Stress distributions along Burgers vector [111] on the slip plane $(1\bar{1}0)$ for initial equilibrium dislocations; a) shear stresses σ_{xy}, b) normal stresses σ_{yy}

ration in Fig. 2a and the stress distribution in Fig. 4b, reveals that the dislocation dissociates into three fractional dislocations which cause three peaks in the normal stress distribution. The width of the dislocation core is about $6a_0$. A dislocation core structure for the $1/2(1\bar{1}0)$ [111] edge dislocation in b.c.c. structures was investigated by Vitek and Yamaguchi [11] with three different potentials, in which the differential displacemental method was used to interpret the dislocation core structure. They reported a very similar dislocation core structure as obtained by the present work. The width of the dislocation core is about $4a_0$ to $6\,a_0$ which depends strongly on the potentials. For the dislocation in the presence of a Cu precipitate, it is seen that the stress distribution at the arm part is essentially the same as that of the pure dislocation, except that the dislocation core is displaced by about 15 Å. However, the stress distribution at the middle part of the dislocation is quite different from that produced by a pure dislocation, which indicates that the dislocation core is no longer symmetric. Because of the structure change of the Cu precipitate, a compressive stress appears on the slip plane in front of the dislocation, and the shear stress on the slip plane decreases. Combining the atomic configuration in Fig. 2b and the shear stress distribution in Fig. 4a, two fractional dislocations can be detected just nearby the interface between the Cu precipitate and Fe matrix. The other fractional dislocation is located inside the Cu precipitate. However, the dislocation core also seems to be planar.

As discussed early in this section, the boundary condition employed in the present work may affect the simulation results when the model size is small. A comparison of dislocation core profiles obtained by different methods shows that this boundary condition has no significant influence on dislocation core profiles. However, we found that normal stress on the slip plane does not tend to zero with increasing distance from the dislocation core. Since this non-zero tensile stress increases the distance between two slipping planes, it decreases the yield stress. Therefore, the boundary conditions employed in this work may yield a lower yield stress.

5. Dislocation Slip

As shown in Fig. 4, the interaction between the metastable b.c.c. Cu precipitate and the dislocation results in a considerable change in stress distributions on the dislocation slip plane, as well as the dislocation core atomic structures. The compressive stress σ_{yy} and the distortion of the atomic structure in front of the dislocation must affect the dislocation slipping behavior, hence, the yield stress. In order to study the strengthening effect of Cu precipitates and the mechanisms of a dislocation passing through the Cu precipitate, a pure shear deformation is applied to a pure Fe single crystal with an edge dislocation, and to a Fe single crystal containing an edge dislocation as well as a Cu precipitate. During the simulation, the average strain components ε_x and ε_z are kept to be zero to satisfy the periodic boundary condition. A displacement increment of $\Delta u_x/L_2 = 0.00075$ to 0.0075 is applied repeatedly to perform a shear deformation. The displacement increment is chosen to be small enough so that the Peierls stress can be obtained. Fig. 5 shows the profiles of the dislocation line on $(1\bar{1}0)$ plane in the initial equilibrium configuration and during the dislocation slip. It is clearly seen that the arm part of the dislocation moves forward (bows out) when the applied stress reaches the Peierls stress, but the middle part of the dislocation is restrained by the Cu precipitate. For the pure dislocation, the profile of the dislocation line remains straight during slipping. The stress distributions on the slip plane at each deformation stage are calculated. Analyzing the change of the maximum and minimum shear stresses on the slip plane for the pure dislocation, it is found that as the applied shear deformation increases, the dislocation starts slipping while the maximum shear stress changes from 0.072 to 0.073 GPa, and the minimum shear stress changes from -0.073 to -0.072 GPa. Fig. 6 presents the shear stress and normal stress distributions on the slip plane at different deformation stages for the pure dislocation. It can be concluded that the change of stress distributions of the pure dislocation core during slipping is very small, i.e. the core structure remains unchanged during slipping. The stress distributions in the presence of a Cu precipitate are shown in Fig. 7. It is found that there is no slip for the fractional dislocation inside the precipitate until the arm part of the dislocation slips

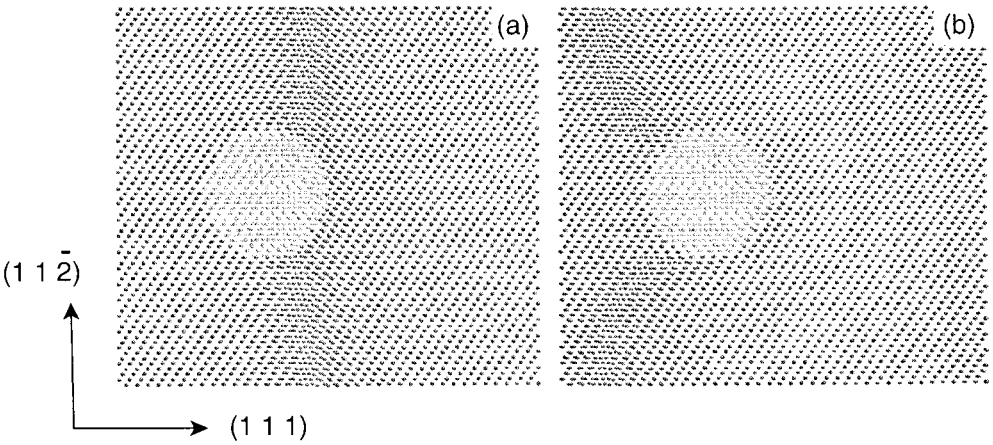

Fig. 5. Profiles of dislocation lines on the slip plane $(1\bar{1}0)$: a) initial equilibrium dislocation, b) slipping dislocation

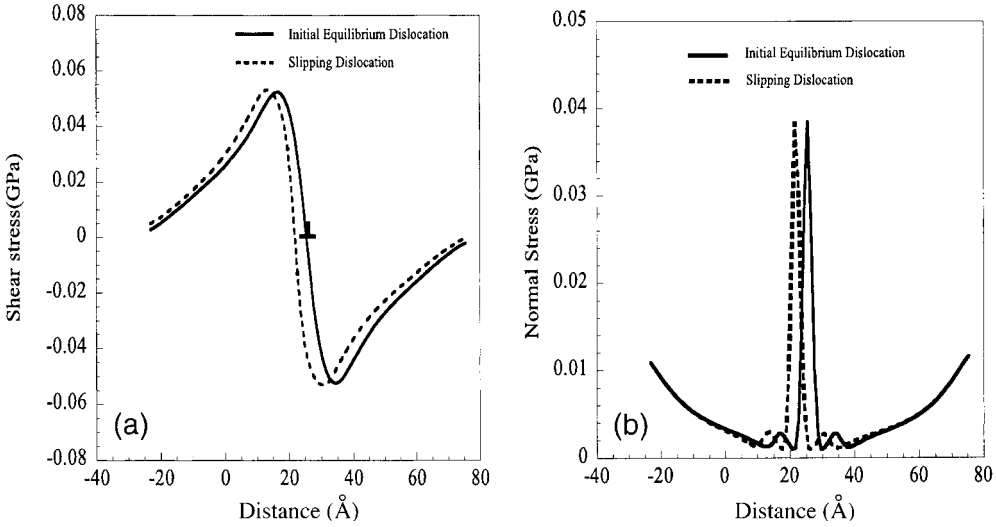

Fig. 6. Stress distributions for the pure dislocation along Burgers vector [111] on the slip plane (110): a) shear stress, b) normal stress

about 40 Å. The maximum shear stress increases and minimum shear stress decreases due to the presence of the precipitate as compared to those for a pure dislocation.

A larger system is used to investigate the whole process of dislocation passing through the Cu precipitate. The average shear stress $\langle \sigma^0_{xy} \rangle$ and average shear strain $\langle \varepsilon^0_{xy} \rangle$ of the whole simulation crystal are calculated. Since the shear deformation is performed by a specified displacement Δu_x, it is easy to get the average strain. The average shear stress is calculated with $\langle \sigma^0_{xy} \rangle = F_x/S$. F_x arises from interactive forces between the active atoms and the atoms in the upper block, and S is the cross section area of the specimen in the x–y plane. The average stress and average strain curves are shown in Fig. 8. The stress–strain curves of the pure dislocation are inserted in Fig. 8 for comparison. The stress at the first significant drop corresponds to the Peierls stress for the pure dislocation. It is shown that the Peierls stress is very small, about 0.01 GPa. A smaller Peierls stress is due to the width increase of dislocation core and tensile stress on the slip plane caused by the boundary condition. However, the presence of the Cu precipitate greatly increases the stress needed to move a dislocation. The yield stress or CRSS in the presence of a Cu precipitate is about 0.5 GPa. We can find that the contribution of the Cu precipitate to the CRSS is obvious. Of course, the CRSS in a real material depends on the precipitate density. The last jump in the stress strain curve indicates that the dislocation completely passed through the precipitate.

Fig. 9 shows the atomic configurations during the dislocation slip process. From Fig. 9, it is found that as the applied shear deformation increases, the arm part of the dislocation slips forward (bows out) continuously. The evolution process of the dislocation line is similar to the Orowan process [5]. However, no dislocation loop is left behind after the dislocation completely by-passes the Cu precipitate. A careful examination of the atomic configuration revealed that the small drop in the final part of the stress–strain curve is related to the dislocation cutting through the precipitate. The cutting process can be demonstrated by comparing the atomic configurations in Cu precipitates in

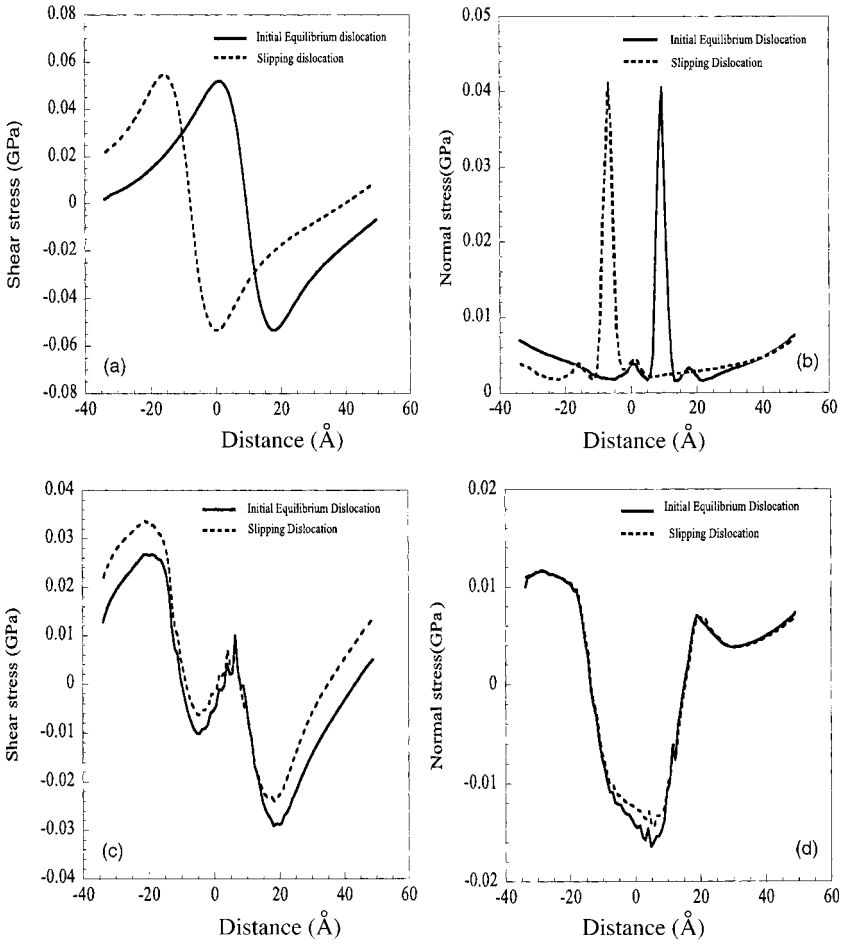

Fig. 7. Shear (left) and normal (right) stress distributions along Burgers vector [111] on the slip plane $(1\bar{1}0)$: a), b) at the arm part ($z = 10\,a_0$) and c), d) at the middle part ($z = 0$), respectively

Fig. 9. After the dislocation cuts through the Cu precipitate, the initially disordered atomic configuration in the precipitate restores order again. In addition, it is also found that a small segment of the dislocation (located between $z = 0$ and $z = 1.5a_0$) switches its original slip plane $(1\bar{1}0)$ ($y = 0$) to the slip plane $(1\bar{1}0)$ ($y = -1.414a_0$) after it completely slips through the precipitate, and then slips forward on that slip plane. The remained defect in the Cu precipitate and the formation of the small dislocation segment are due to structural transformations. Therefore, our results suggest that a dislocation passes through a Cu precipitate by a cutting mechanism.

From the entire atomic structural evolution presented above, it is clear that in order to get quantitative results of CRSS in Fe matrix with Cu precipitates, the contribution to CRSS from lattice mismatch and the internal stresses caused by Cu precipitate phase transformation should be considered, in addition to the modulus mismatch and the precipitate density. Because of the influence of boundary conditions, a smaller Peierls stress for a pure dislocation was obtained in the present simulation model. To improve

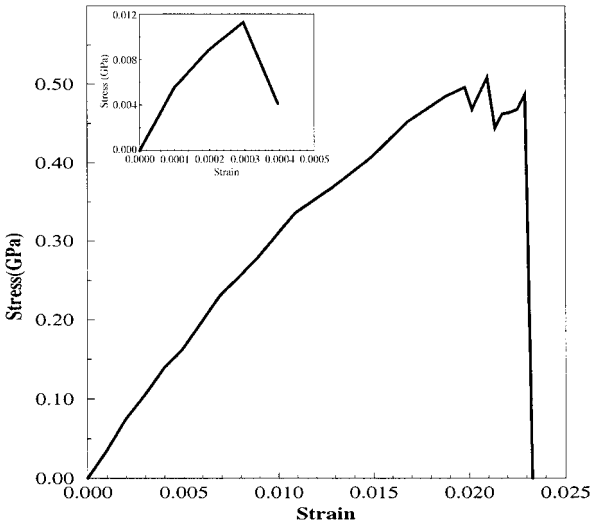

Fig. 8. Average shear stress–strain curve for the b.c.c. Fe single crystal with a Cu precipitate and an edge dislocation under shear deformation (insert shows the same for the pure dislocation)

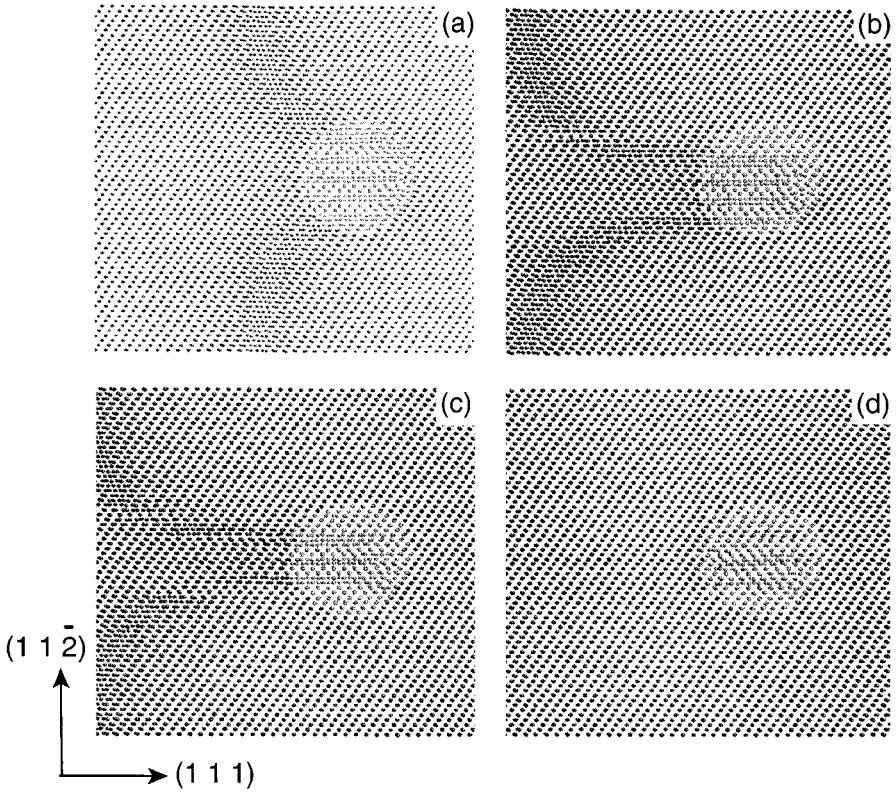

Fig. 9. Profiles of the dislocation lines on the slip plane $(1\bar{1}0)$ at different deformation stages, the applied average strains are: a) 0.005, b) 0.02, c) 0.023 and d) 0.0235

accuracy in calculating the yield stress, one may consider other boundary conditions in the future, such as the flexible boundary condition [22].

6. Conclusion

The interactions between an edge dislocation and a Cu precipitate in b.c.c. Fe have been studied by molecular static calculations. The core structures of the dislocation are interpreted by mapping the atomic stress distributions on the slip plane. For the pure dislocation core structures and its slip behavior, good agreement between our calculations and previous atomistic simulation results is obtained. Because of the interaction between the Cu precipitate and the dislocation, a similar b.c.c. to 9R structure transformation occurs in the metastable b.c.c. Cu precipitate, which results in a considerable change in stress distributions on the dislocation slip plane, as well as the dislocation core atomic structures. The compressive stress σ_{yy} and the distortion of atomic structure in front of the dislocation restrain the dislocation from slipping forward. Consequently, the CRSS is increased greatly. Furthermore, it is found that the motion of the dislocation line is similar to the Orowan process. However, no dislocation loop is left behind after the dislocation completely by-passes the Cu precipitate. From the analysis of the evolution of atomic configurations in the Cu precipitate, it is suggested that a cutting mechanism is operative when the dislocation passes through the precipitate.

Acknowledgements The authors are grateful for the partial support from the National Science Foundation under the grant number DMR-96-33719. Some of the simulations were performed at the San Diego Supercomputer Center and the Pittsburgh Supercomputing Center.

References

[1] P. J. Othen, M. L. Jenkins, and G. D. W. Smith, Phil. Mag. A **73**, 249 (1996).
[2] S. Pizzini, K. J. Robert, W. J. Phythian, C. A. English, and G. N. Greaves, Phil. Mag. Lett. **61**, 223 (1990).
[3] W. J. Phythian, A. J. E. Foreman, C. A. English, J. Buswell, T. M. Hetherington, K. Roberts, and S. Pizzini, AEA Technology Harwell Rep. AEA-TRs-2004 (1990).
[4] S. Y. Hu, Y. L. Li, and K. Watanabe, Modelling Simul. Mater. Sci. Eng. **7**, 641 (1999).
[5] E. Nembach, Particle Strengthening of Metals and Alloys, Wiley Interscience, New York 1997.
[6] F. J. Humphreys, Dislocation-Particle Interactions, in: Dislocations and Properties of Real Materials, The Institute of Metals, London 1985.
[7] F. R. N. Nabarro, Dislocation in Solids, Vol. 8, 1989.
[8] Z. S. Basinski, M. S. Duesbery, and R. Taylor, Canad. J. Phys. **49**, 2160 (1971).
[9] J. O. Schiffgens and K. E. Garrison, J. Appl. Phys. **43**, 3240 (1971).
[10] M. Yamaguchi and V. Vitek, J. Phys. F **3**, 523 (1973).
[11] V. Vitek and M. Yamaguchi, J. Phys. F **3**, 532 (1973).
[12] B. L. Adams, J. P. Hirth, P. C. Gehlen, and R. G. Hoagland, J. Phys. F **7**, 2021 (1977).
[13] R. Schroll, P. Gumbsch, and V. Vitek, Mater. Sci. Engng. A **233**, 116 (1997).
[14] G. Simonnelli, R. Pasionot, and E. J. Savino, Mater. Res. Soc. Symp. Proc. **291**, 567 (1993).
[15] A. F. Voter, Los Alamos Unclassified Technical Report 93-3901, Los Alamos National Laboratory, 1993.
[16] M. Ludwig, D. Farkas, D. Pedraza, and S. Schmauder, Modelling Simul. Mater. Sci. Eng. **6**, 19 (1998).
[17] G. R. Hoagland, M. R. Daw, S. M. Foiles, and M. I. Baskes, J. Mater. Res. **5**, 313 (1990).
[18] R. G. Hoagland, M. S. Daw, and J. P. Hirth, J. Mater. Res. **6**, 2565 (1991).
[19] M. Ahlers, Z. Metallk. **65**, 636 (1974).
[20] S. Kajiwara, Trans. Japan Inst. Metals **17**, 435 (1976).
[21] Yu. N. Osetsky and A. Serra, Phil. Mag. A **73**, 249 (1996).
[22] S. Kohlhoff and S. Schmauder, Atomistic Simulation of Materials, Eds. V. Vitek and D. J. Srolovitz, Plenum Press, New York 1989.